J. Fluid Mech. (1969), *vol.* 35, *part* 3, *pp.* 497–525
Printed in Great Britain

Lee waves in a stratified flow. Part 4. Perturbation approximations

By JOHN W. MILES† AND HERBERT E. HUPPERT†

Institute of Geophysics and Planetary Physics,
University of California, La Jolla

(Received 9 May 1968)

A two-dimensional stratified flow over an obstacle in a half space is considered on the assumptions that the upstream dynamic pressure and density gradient are constant (Long's model). A general solution of the resulting boundary-value problem is established in terms of an assumed distribution of dipole sources. Asymptotic solutions for prescribed bodies are established for limiting values of the slenderness ratio ϵ (height/breadth) of the obstacle and the reduced frequency k (inverse Froude number based on the obstacle breadth) as follows: (i) $\epsilon \to 0$ with k fixed; (ii) $k \to 0$ with ϵ fixed; (iii) $k \to \infty$ with $k\epsilon$ fixed. The approximation (i) is deveoped to both first (linearized theory) and second order in ϵ in terms of Fourier integrals. The approximation (ii), which constitutes a modification of Rayleigh-scattering theory, is obtained by the method of matched asymptotic expansions and depends essentially on the *dipole form* (which is proportional to the sum of the displaced and virtual masses) of the obstacle with respect to a uniform flow. A simple approximation to this dipole form is proposed and validated by a series of examples in an appendix. The approximation (iii) is obtained through the reduction of the original integral equation to a singular integral equation of Hilbert's type that is solved by the techniques of function theory. A composite approximation to the lee-wave field that is valid in each of the limits (i)–(iii) also is obtained. The approximation (iii) yields an estimate of the maximum value of $k\epsilon$ for which completely stable lee-wave formation behind a slender obstacle is possible. The differential and total scattering cross-sections and the wave drag on the obstacle are related to the power spectrum of the dipole density. It is shown that the drag is invariant under a reversal of the flow in the limits (i) and (ii), but only for a symmetric obstacle in the limit (iii). The results are applied to a semi-ellipse, an asymmetric generalization thereof, the Witch of Agnesi (Queney's mountain), and a rectangle. The approximate results for the semi-ellipse are compared with the more accurate results obtain by Huppert & Miles (1969). It appears from this comparison that the approximate solutions should be adequate for any slender obstacle within the range of $k\epsilon$ for which completely stable lee-wave formation is possible. The extension to obstacles in a channel of finite height is considered in an appendix.

† Also Department of Aerospace and Mechanical Engineering Sciences.

1. Introduction

We continue our investigation of the generation of lee waves by, the consequent drag on, and the parametric range of (statistically) stable flow for an obstacle in a two-dimensional, steady, inviscid, stratified shear flow in which the upstream dynamic pressure and density gradient are regarded as constant (Long's model). In part 1 (Miles 1968*a*), we considered a thin barrier in either a channel of finite height or a half space. In part 2 (Miles 1968*b*), we considered a semi-circular obstacle in a half space. In part 3 (Huppert & Miles 1969), we extended the latter analysis to a semi-elliptical barrier. We refer to these papers subsequently as I, II, and III, followed by the appropriate equation number therefrom. We consider here an arbitrary cylindrical obstacle, say C, of characteristic base length b and height h in a half space and give asymptotic solutions for limiting values of one or more of the parameters

$$\epsilon = h/b, \quad k = Nb/U, \quad \kappa = k\epsilon = Nh/U, \tag{1.1a, b, c}$$

where N is the intrinsic (Väisälä) frequency and U is the wind speed of the basic flow; we consider the necessary modifications for a channel of finite height in

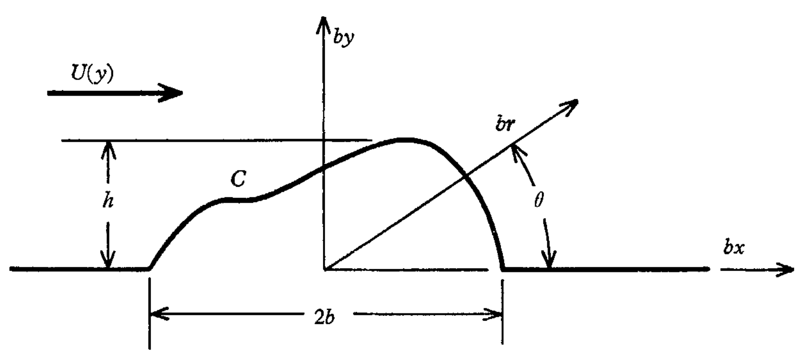

FIGURE 1. Finite obstacle in semi-infinite, stratified flow.

appendix B. We require both the height and the cross-sectional area, say A, of the obstacle to be finite and define b as half the base length, if finite, or as proportional to A/h if the base length is infinite.

Let x and y be dimensionless, Cartesian co-ordinates with b as the unit of length, r and θ the corresponding polar co-ordinates (see figure 1),

$$y = \epsilon\eta(x) \tag{1.2}$$

the description of the lower boundary ($\eta \equiv 0$ outside of C), and $h\delta(x, y)$ the vertical displacement of a given streamline relative to its horizontal trace in the basic flow; then Long's model yields the following boundary-value problem for the half-space:

$$\nabla^2\delta + k^2\delta = 0, \tag{1.3}$$

$$\delta(x, \epsilon\eta) = \eta(x), \tag{1.4}$$

and

$$\delta(x, y) = o(r^{-\frac{1}{2}}) \quad (x \to -\infty). \tag{1.5}$$

Long's model also requires

$$\epsilon\delta_y \leqslant 1 \tag{1.6}$$

at every point in the flow as a necessary condition for static stability ($\epsilon\delta_y > 1$ implies that the vertical gradient of the density is locally positive and that the flow is locally reversed).

Lyra's model of a uniform flow (no shear) in an isothermal atmosphere also leads to the boundary-value problem posed by (1.3)–(1.5) *if* the Boussinesq approximation and the restriction to infinitesimal disturbances also are invoked (Lyra 1943; Queney 1948; Yih 1965, pp. 66–74). The restriction (1.6) then is satisfied by hypothesis.

We give a general solution of (1.3) and (1.5) in §2 below in terms of a distribution of dipole sources along the base of the obstacle. Invoking (1.4) then yields a linear integral equation for the density of this distribution. We consider the determination of this density in the following limits: (i) $\epsilon \to 0$ with k fixed; (ii) $k \to 0$ with ϵ fixed; (iii) $k \to \infty$ with κ fixed. Only (i) is relevant for Lyra's model.

The limit $\epsilon \to 0$ yields the *planar approximation* (we also use the adjectives *first-order* and *linearized* to describe this approximation), in which the left-hand side of (1.4) is approximated by $\delta(x, 0+)$. The resulting solution is due essentially to Lyra (1943) and Queney (1948), who gave solutions for a rectangle and the Witch of Agnesi, respectively, on the hypotheses of Lyra's model. The extension to an arbitrary configuration follows by linear superposition. The calculation of the drag in this approximation appears to be due originally to Blumen (1965).

The limit $k \to 0$ permits the Helmholtz equation (1.3) to be approximated by Laplace's equation in the neighbourhood of C and the field at large distances from C ($kr \to \infty$) to be represented by a single dipole source, the strength of which may be determined by solving the problem of uniform irrotational flow over C. The corresponding procedure in diffraction theory is known as the *Rayleigh-scattering* approximation (Rayleigh 1897), and it seems appropriate to extend that description in the present context. We give the details in §4 and show that the limiting representations of the scattering cross-section and the drag (defined in §3) as $k \to 0$ are proportional to the square of the *dipole form* of C with respect to a uniform, horizontal flow and are otherwise independent of C. We also give a simple approximation to this dipole form that depends only on the area and height of the obstacle and appears to be fairly accurate for a wide variety of cross-sections.

The first-order approximation is not uniformly valid as $k \to \infty$ in consequence of the implicit assumption $k\epsilon \ll 1$. We are therefore led to investigate the asymptotic limit $k \to \infty$ with κ fixed. We find (in §5) that the integral equation for the dipole density then reduces to a singular integral equation of Hilbert's type, which we solve by invoking known techniques of function theory. This solution has the happy property of reducing to the first-order solution in the limit (i) and therefore provides a uniformly valid (with respect to k) approximation for small ϵ.

We also infer from this asymptotic solution that the upper bound on κ implied by the constraint (1.6), say κ_c, is less than one. This suggests that the asymptotic approximation may be expanded in κ, and we find that it typically suffices to neglect terms of $O(\kappa^3)$ relative to unity for $\kappa < \kappa_c$. [The formulation of §5 is meaningful, and the conclusion $\kappa_c < 1$ valid, only for $\epsilon \ll 1$. We recall (see III) that κ_c increases monotonically from 0·7 to 1·7 for a semi-elliptical obstacle as ϵ increases from 0 to ∞.]

We return to the limit (i) in §6 and obtain a second-order (in ϵ) approximation to the dipole density by expanding (1.4) about $\epsilon = 0$ on the hypothesis that the obstacle is continuous (as a rectangular obstacle, for example, is *not*). The limiting form of this approximation as $k \to 0$ is especially simple and provides a second-order approximation to the dipole form that appears to be superior (even for non-small ϵ) to the simpler approximation given in §4 for smooth obstacles.

We apply the results of §§2–6 to a semi-ellipse and an asymmetric generalization thereof in §7, the Witch of Agnesi in §8, and a rectangle in §9. The various Fourier and Hilbert transforms that enter the calculations in these last sections may be found in the tables of Erdélyi, Magnus, Oberhettinger & Tricomi (1953*b*).

2. General solution

We pose a general solution to (1.3) in the alternative forms

$$\delta(x,y) = \pi^{-1}\int_{-\infty}^{\infty} f(\xi)\,\delta_1(x-\xi,y)\,d\xi \tag{2.1a}$$

$$= \mathscr{R}\int_{0}^{\infty} F(\alpha)\exp\{i\alpha x-(\alpha^2-k^2)^{\frac{1}{2}}y\}\,d\alpha, \tag{2.1b}$$

where
$$\delta_1(x,y) = \mathscr{R}\int_{0}^{\infty}\exp\{i\alpha x-(\alpha^2-k^2)^{\frac{1}{2}}y\}\,d\alpha \tag{2.2}$$

is (we anticipate) a dipole solution of (1.3), $f(x)$ is the equivalent dipole density of the obstacle,

$$\pi F(\alpha) = \int_{-\infty}^{\infty} f(\xi)\exp(-i\alpha\xi)\,d\xi \tag{2.3}$$

is its Fourier transform (the factor π proves convenient in the subsequent development), and the operator $\mathscr{R}$ yields the real part of its operand. Letting $y \to 0$ in (2.1*a*, *b*) and invoking Fourier's integral formula, we obtain

$$\delta(x,0+) = f(x), \quad \delta_1(x,0+) = \pi\hat{\delta}(x), \tag{2.4a, b}$$

where $\hat{\delta}(x)$ is Dirac's delta function. We infer from (2.4*a*) that $f(x) \equiv 0$ outside of C; accordingly, we may replace the limits of integration in (2.1*a*) and (2.3) by ± 1 for an obstacle of finite base $2b$ with its mid-point at $x = 0$. It remains possible that $f(x) = 0$ over some finite portion of $x = (-1, 1)$, as in the neighbourhood of a blunt end (see below).

Invoking the boundary condition (1.4) in (2.1*a*) yields an integral equation for $f(x)$. We consider the solution of this integral equation in §§5 and 6 below (and, implicitly, in §4), but note here that the solution in the planar approximation follows directly from (2.4*a*):

$$f(x) \to \eta(x) \quad (\epsilon \to 0) \tag{2.5}$$

provided that $\eta'(x)$ is uniformly bounded. The approximation is not uniformly valid in the neighbourhood of a stagnation point (where $\eta' \to \infty$), but a uniformly valid solution may be obtained by regarding the flow as potential within a radius of $O(1/k)$ of such a point. For example, a uniformly valid, linearized approximation for the semi-ellipse $\eta(x) = (1-x^2)^{\frac{1}{2}}$ is given by $f(x) = (1-\epsilon^2-x^2)^{\frac{1}{2}}$, with $f(x) \equiv 0$ in the intervals between the foci at $x = \pm(1-\epsilon^2)^{\frac{1}{2}}$ and the stagnation points at $x = \pm 1$.

Considering next the requirement (1.5), we find that a stationary-phase approximation to (2.2) on the hypothesis (Queney 1948) that the path of integration passes under the branch point at $\alpha = k$ yields

$$\delta_1(x,y) \sim H(x)(2\pi k/r)^{\frac{1}{2}}\cos(kr-\tfrac{1}{4}\pi)\sin\theta\{1+O(1/kr)\}+O(1/x) \quad (kr\to\infty), \tag{2.6}$$

where

$$H(x) = \{0, \tfrac{1}{2}, 1\} \quad (x<0, x=0, x>0) \tag{2.7}$$

is Heaviside's step function. We conclude that (1.5) is satisfied for the assumed path of integration and that the alternative choice of a path over the branch point would have yielded upstream, rather than downstream, waves.

Replacing x by $x-\xi$ and r by

$$R = \{(x-\xi)^2+y^2\}^{\frac{1}{2}} \tag{2.8a}$$

$$\sim r-\xi\cos\theta+O(r^{-1}) \quad (r\to\infty) \tag{2.8b}$$

in (2.6), substituting the dominant term in the result into (2.1*a*), and invoking (2.3), we obtain the asymptotic lee-wave field in the alternative forms

$$\delta(x,y) \sim (2k/\pi r)^{\frac{1}{2}}\sin\theta H(\tfrac{1}{2}\pi-\theta)\int_{-\infty}^{\infty} f(\xi)\cos\{k(r-\xi\cos\theta)-\tfrac{1}{4}\pi\}d\xi \quad (r\to\infty) \tag{2.9a}$$

$$= (2\pi k/r)^{\frac{1}{2}}\sin\theta H(\tfrac{1}{2}\pi-\theta)\mathscr{R}\{F(k\cos\theta)\exp[i(kr-\tfrac{1}{4}\pi)]\}. \tag{2.9b}$$

[The presence of $H(x)$ in (2.6) implies that the upper limit on the integral of (2.9*a*) should be x, rather than ∞; however, the difference is negligible, either because of the finite breadth of the obstacle or because of the restriction to obstacles of finite cross-sectional area, which implies that the contribution of the range (x,∞) to the integral is asymptotically negligible.] We remark that the lee-wave field given by (2.9) is transverse in the sense that the radial and tangential components of the velocity field, $\epsilon U\{-r^{-1}\delta_\theta, \delta_r\}$ relative to the basic flow, are $O(k^{\frac{1}{2}}r^{-\frac{3}{2}})$ and $O(k^{\frac{3}{2}}r^{-\frac{1}{2}})$, respectively, as $kr\to\infty$.

We now go on to consider additional representations of δ_1 and to confirm its dipole character. Introducing the changes of variable

$$\alpha = k\cos t \quad (0\leqslant\alpha<k) \tag{2.10a}$$

$$= k\cosh t \quad (\alpha>k) \tag{2.10b}$$

in (2.2) and invoking the identity [Erdélyi, Magnus, Oberhettinger & Tricomi 1953*a*, §7.12(18) after replacing x and y therein by y and ix, respectively]

$$\pi Y_1(kr)\exp[i(\tfrac{1}{2}\pi-\theta)] = \int_0^\pi \exp(ikx\cos t)\sin(ky\sin t-t)\,dt$$
$$-2\int_0^\infty \exp[-ky\sinh t]\sinh(ikx\cosh t+t)\,dt, \tag{2.11}$$

where r and θ are the polar co-ordinates, we obtain the alternative representations

$$\delta_1(x,y) = k\int_0^{\frac{1}{2}\pi} \cos\{k(x\cos t + y\sin t)\}\sin t\,dt + k\int_0^\infty \exp(-ky\sinh t)\cos(kx\cosh t)\sinh t\,dt \quad (2.12a)$$

$$= -\tfrac{1}{2}\pi k Y_1(kr)\sin\theta - k\int_0^{\frac{1}{2}\pi} \sin(kx\cos t)\sin(ky\sin t)\sin t\,dt. \quad (2.12b)$$

Comparing (2.12 b) with II (2.1) and II (2.7), we find that δ_1 is identical with the first of the complete set of functions, $\{\delta_n\}$, determined in II and has the Fourier-series representation†

$$\delta_1(r\cos\theta, r\sin\theta) = -\tfrac{1}{2}\pi k Y_1(kr)\sin\theta - 4k\sum_{m=1}^{\infty} m(4m^2-1)^{-1}J_{2m}(kr)\sin 2m\theta. \quad (2.13)$$

Letting $kr \to 0$, we obtain

$$\delta_1(r\cos\theta, r\sin\theta) = r^{-1}\sin\theta\{1 + O(k^2r^2\log kr)\} \quad (kr\to 0), \quad (2.14)$$

which identifies δ_1 as a dipole solution of (1.3) and (1.5).

We construct a related set, say $\{\hat{\delta}_n\}$, by differentiation, such that $\hat{\delta}_n$ exhibits a *2n-pole* behaviour as $r \to 0$:

$$\hat{\delta}_n(x,y) = (-\partial/\partial x)^{n-1}\{\delta_1(x,y)/(n-1)!\} \quad (2.15a)$$

$$\to r^{-n}\sin n\theta\{1 + O(k^2r^2)\} \quad (kr\to 0) \quad (2.15b)$$

$$\sim H(x)(2\pi k/r)^{\frac{1}{2}}\sin\theta\,\mathscr{R}\{(-ik\cos\theta)^{n-1}\exp[i(kr-\tfrac{1}{4}\pi)]\} \times\{1 + O(1/kr)\} \quad (kr\to\infty). \quad (2.15c)$$

The set $\{\hat{\delta}_n\}$ is complete in $\theta = (0,\pi)$ for fixed r, and each of the $\hat{\delta}_n$ satisfies (1.3) and (1.5). [The set $\{\delta_n(r,\theta)\}$ in II also has these properties, and $\delta_n \to \hat{\delta}_n$ in each of the limits of (2.15 b, c); the two sets are linearly dependent, but not identical.] We expand $\delta(x,y)$ in the $\hat{\delta}_n$ by expanding $\delta_1(x-\xi, y)$ in a Taylor series about $\xi = 0$ in (2.1 a):

$$\delta(x,y) = \sum_{n=1}^{\infty} F_{n-1}\hat{\delta}_n(x,y), \quad (2.16)$$

where

$$F_n = \pi^{-1}\int_{-\infty}^{\infty} \xi^n f(\xi)\,d\xi \quad (2.17a)$$

$$= \{(i\partial/\partial\alpha)^n F(\alpha)\}_{\alpha=0} \quad (2.17b)$$

is the nth moment of $f(x)$. We designate F_0 as the *dipole moment*; see §4 below. All of the F_n exist for a finite obstacle. but not, in general, for an infinite obstacle; e.g. the representation (2.16) is not possible for the Witch of Agnesi (§8 below).

† The dipole solution (2.13) appears to have been given originally by Lyra (1943) in connexion with the problems of a plateau and a rectangular obstacle in the context of the model described in §1.

We obtain still another representation of δ_1 by taking the Fourier-sine transform of (1.3) with respect to y, invoking (2.4*b*) at $y = 0$, and then requiring the transform to satisfy (1.5). The result is

$$\delta_1(x,y) = -2H(x)\int_0^k \nu(k^2-\nu^2)^{-\frac{1}{2}}\sin\{(k^2-\nu^2)^{\frac{1}{2}}x\}\sin\nu y\,d\nu + \int_k^\infty \nu(\nu^2-k^2)^{-\frac{1}{2}}\exp\{-(\nu^2-k^2)^{\frac{1}{2}}|x|\}\sin\nu y\,d\nu, \quad (2.18)$$

where $H(x)$ is given by (2.7).

3. Scattering cross-sections and drag

The differential scattering cross-section of the obstacle is given by [II (1.8*a*)]

$$\sigma(\theta) = \epsilon^2 b \lim_{r\to\infty} r(\delta_r^2 + k^2\delta^2) \quad (3.1a)$$

$$= 2\pi\epsilon^2 k^3 b|F(k\cos\theta)|^2 \sin^2\theta H(\tfrac{1}{2}\pi-\theta), \quad (3.1b)$$

where (3.1*b*) follows from (3.1*a*) by virtue of (2.9*b*). The ratio of the energy density in the scattered lee wave to that in the basic flow is $\sigma(\theta)/br$. The total scattering cross-section is given by

$$Q = \int_0^{\frac{1}{2}\pi}\sigma(\theta)\,d\theta \quad (3.2a)$$

$$= 2\pi\epsilon^2 kb\int_0^k |F(\alpha)|^2(k^2-\alpha^2)^{\frac{1}{2}}d\alpha. \quad (3.2b)$$

The lee-wave drag is given by [II (1.10*b*)]

$$D \equiv qhC_D = q\int_0^{\frac{1}{2}\pi}\sigma(\theta)\cos\theta\,d\theta \quad (3.3a)$$

$$= 2\pi\epsilon qh\int_0^k |F(\alpha)|^2(k^2-\alpha^2)^{\frac{1}{2}}\alpha\,d\alpha, \quad (3.3b)$$

where $q = \frac{1}{2}\rho U^2$ and ρ are the dynamic pressure and density in the basic flow. The result (3.3*b*) was given by Sawyer (1959) and Blumen (1965) in the context of Lyra's model.

The function $|F(\alpha)|^2$ is essentially the power spectrum of the dipole-distribution function $f(x)$. Invoking (2.3), integrating by parts, and invoking the implicit requirements that $|F(\alpha)|^2$ be real and that $f(\pm\infty)$ vanish, we obtain the alternative representations

$$|\pi F(\alpha)|^2 = \int_{-\infty}^{\infty}\int_{-\infty}^{\infty} f(x)f(\xi)\cos\{\alpha(x-\xi)\}\,dx\,d\xi \quad (3.4a)$$

$$= \alpha^{-1}\int_{-\infty}^{\infty}\int_{-\infty}^{\infty} f(x)f'(\xi)\sin\{\alpha(x-\xi)\}\,dx\,d\xi \quad (3.4b)$$

$$= \left\{\pi\sum_{m=0}^{\infty}(-)^m F_{2m}\alpha^{2m}/(2m)!\right\}^2 + \left\{\pi\sum_{m=0}^{\infty}(-)^m F_{2m+1}\alpha^{2m+1}/(2m+1)!\right\}^2. \quad (3.4c)$$

The last representation may not be valid for infinite obstacles. Substituting (3.4a) and (3.4b) into (3.2b) and (3.3b), respectively, and invoking the integral representations

$$J_1(x) = (2x/\pi)\int_0^1 (1-t^2)^{\frac{1}{2}}\cos xt\,dt \tag{3.5}$$

and

$$\mathbf{H}_1(x) = (2x/\pi)\int_0^1 (1-t^2)^{\frac{1}{2}}\sin xt\,dt \tag{3.6}$$

for the Bessel function J_1 and the Struve function $\mathbf{H}_1$, we obtain

$$Q = \kappa^2 b\int_{-\infty}^{\infty}\int_{-\infty}^{\infty}(x-\xi)^{-1}J_1\{k(x-\xi)\}f(x)f(\xi)\,dx\,d\xi \tag{3.7}$$

and

$$C_D = \kappa\int_{-\infty}^{\infty}\int_{-\infty}^{\infty}(x-\xi)^{-1}\,\mathbf{H}_1\{k(x-\xi)\}f(x)f'(\xi)\,dx\,d\xi. \tag{3.8}$$

Substituting (3.4c) into (3.2b) and (3.3b), we obtain the power series

$$Q = \tfrac{1}{2}\pi^2\epsilon^2k^3b\{F_0^2+\tfrac{1}{4}(F_1^2-F_0F_2)k^2+\ldots\} \tag{3.9}$$

and

$$D = \tfrac{2}{3}\pi\epsilon^2k^3qb\{F_0^2+\tfrac{2}{5}(F_1^2-F_0F_2)k^2+\ldots\}. \tag{3.10}$$

The representations of (3.7) and (3.8) are especially convenient for large k (see §5 below), whereas those of (3.9) and (3.10) are especially convenient for small k (see §4 below) provided that the F_n are finite.

We infer from (3.3b) that C_D/k is a monotonically increasing function of k for prescribed $|F(\alpha)|^2$ (as in the planar approximation) and tends to a finite limit as $k\to\infty$ if $|F(\alpha)| = o(\alpha^{-\frac{1}{2}})$ as $\alpha\to\infty$ [a condition that is satisfied if $\eta(x)$ is continuous, but is violated by a rectangular obstacle; see (9.2c) below]. We infer from the latter result that the planar approximation to D vanishes like U as $U\to 0$ for fixed N and therefore (since D vanishes like $1/U$ as $U\to\infty$ for fixed N) exhibits a maximum with respect to U at some finite value of U. This conclusion is, however, of limited significance in consequence of the nonlinear increase in dC_D/dk as $k\to\infty$, which implies that D would tend to infinity as $U\to 0$ *if* the basic model were valid for $\kappa > \kappa_c$.

Reverse-flow theorem

We remark that both Q and D are invariant under the transformation

$$f(x)\to f(-x).$$

Observing that $\eta(x)\to\eta(-x)$ is equivalent to a reversal of the basic flow, we infer that the planar approximations to both Q and D are invariant under such a reversal independently of the symmetry of the obstacle. We anticipate that this reverse-flow theorem holds also for $k\to 0$ with ϵ fixed (see §4 below). It does not hold for $k\to\infty$ with κ fixed (see §5 below) unless the obstacle is symmetric, i.e. unless $\eta(x)\equiv\eta(-x)$.

4. Rayleigh-scattering approximation ($k \to 0$)

Letting $k \to 0$ in (2.15*b*) and (2.15*c*) and substituting the results into (2.16), we obtain the inner and outer asymptotic approximations

$$\delta(x,y) \sim \sum_{n=1}^{\infty} F_{n-1} r^{-n} \sin n\theta \{1 + O(k^2 r^2 \log kr)\} \quad (kr \to 0) \tag{4.1a}$$

$$\sim F_0 H(x)(2\pi k/r)^{\frac{1}{2}} \sin\theta \cos(kr - \tfrac{1}{4}\pi) \quad (kr \to \infty). \tag{4.1b}$$

It would be consistent with the error in (4.1*a*) to retain both the dipole and the quadrupole terms in (4.1*b*); however, the contribution of the latter term to Q and C_D in the subsequent development would be negligible within the approximation already inplicit in the determination of F_0 on the basis of potential flow.

The expansion (4.1*a*) typically diverges in $r < 1$ and cannot be used to determine the F_n directly from the boundary condition at the body. We therefore require an appropriate continuation of (4.1*a*). The flow in the neighbourhood of the body is potential by virtue of the reduction of Helmholtz's equation (1.3) to Laplace's equation as $k \to 0$ with r fixed. Let

$$\psi(x,y) = y - \epsilon\delta(x,y) \tag{4.2}$$

be the corresponding stream function,

$$w(z) = \phi + i\psi \quad (z = re^{i\theta}) \tag{4.3}$$

the corresponding, complex potential, and C^* the reflexion of C in $y = 0$. Then, if $w(z)$ can be determined such that

$$\psi = 0 \quad \text{on} \quad C + C^*, \tag{4.4}$$

δ satisfies (1.4), and the F_n are determined uniquely by the analytical continuation

$$w(z) = z + \epsilon \sum_{n=1}^{\infty} F_{n-1} z^{-n}, \tag{4.5}$$

the imaginary part of which yields (4.1*a*) after invoking (4.2). The F_n are real by virtue of the symmetry of $C + C^*$ with respect to $y = 0$.

Letting $k \to 0$ in (3.9) and (3.10) and introducing

$$A_1 = (bh/\pi)\int_{-\infty}^{\infty} f(\xi)\,d\xi = bhF_0, \tag{4.6}$$

we obtain
$$Q = \tfrac{1}{2}\pi^2\epsilon^2 F_0^2 k^3 b = \tfrac{1}{2}\pi^2 A_1^2 (N/U)^3 \tag{4.7}$$

and
$$D = \tfrac{2}{3}\pi\epsilon^2 F_0^2 k^3 qb = \tfrac{1}{3}\pi A_1^2 \rho N^3 U^{-1} \tag{4.8}$$

within error factors of $1 + O(k^2 \log k)$.

The parameter A_1 is the *dipole form* of C with respect to a uniform, horizontal, potential flow and has the following, general properties (Pölya 1947; Pölya & Szegö 1951, Note G; see also Lamb 1932, §72*a*): (i) A_1 is invariant under a reversal of the flow; (ii) A_1 is a monotonically increasing set-function of C, such that

$$A_1(C_i) < A_1(C) < A_1(C_0) \quad \text{if} \quad C_i \subset C \subset C_0; \tag{4.9}$$

(iii) A_1 is the sum of the displaced and virtual masses associated with A_1:

$$A_1 = (A+M)/\pi, \tag{4.10}$$

where
$$M = \iint |(dw/dz)-1|^2 dS, \tag{4.11}$$

and the integration is over the exterior of C (note that M has the dimensions of area).

The dipole form for a semi-ellipse of base $2b$ and height h is given by (Lamb 1932, §72a)

$$A_1 = \tfrac{1}{2}h(b+h). \tag{4.12}$$

	Obstacle	A_1	$\lvert (A_*/A_1)-1 \rvert$ $\left[A_* = \dfrac{A}{\pi}+\tfrac{1}{2}h^2\right]$
Thin plate	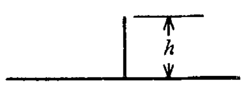	$\tfrac{1}{2}h^2$	0
Semi-ellipse	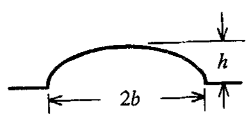	$\tfrac{1}{2}h(b+h)$	0
Circular-arc	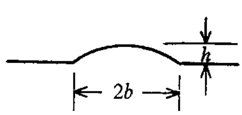	$\dfrac{\alpha(2-\alpha)}{3(1-\alpha)^2}b^2$ $\alpha = \dfrac{2}{\pi}\tan^{-1}\dfrac{h}{b}$	$<0{\cdot}1$ $(0<\alpha<1)$
Full circle	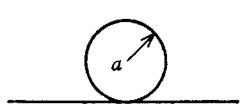	$\tfrac{1}{3}\pi^2 a^2$	0·1
Semi-circular ditch		$-\tfrac{5}{27}a^2$	—
Rectangle		See (A 5)–(A 8)	$<0{\cdot}2$
Lemniscate		$2h^2$	0·1
Joukowsky profile	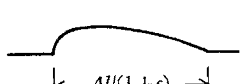	$\epsilon(2-\epsilon)l^2$	$<0{\cdot}1$
Finned semi-circle	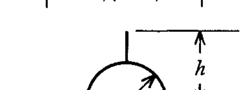	$\dfrac{1}{2}\left(h^2+\dfrac{a^4}{h^2}\right)$	$<0{\cdot}2$

TABLE 1. The dipole form, A_1, for various obstacles, as considered in appendix A.

Using this result in conjunction with (4.9), we obtain the following bounds to A_1 by constructing inscribed and circumscribed semi-ellipses, with semi-axes b_i, h_i and b_0, h_0

$$A_{1i} \equiv \tfrac{1}{2}h_i(b_i+h_i) \leqslant A_1 \leqslant \tfrac{1}{2}h_0(b_0+h_0) \equiv A_{10}. \tag{4.13}$$

These bounds are valid for arbitrary C, but we expect them to be useful primarily for convex C.

The result (4.12) also suggests the semi-empirical approximation

$$A_1 \doteqdot A_* \equiv \pi^{-1}A + \tfrac{1}{2}h^2 \tag{4.14}$$

for any finite obstacle of height h. This approximation evidently is equivalent to the approximation of M by the virtual mass of a semi-circle having the same height, that is

$$M \doteqdot M_* \equiv \tfrac{1}{2}\pi h^2, \tag{4.15}$$

as is exactly true for a semi-ellipse. The examples given in appendix A and summarized in table 1 suggest that (4.14) is a fairly good approximation in general, but that (4.15) may not be correspondingly good. In particular, we find that $M = O[h^2 \log(b/h)]$ for a rectangle of base $2b$ and height h as $h/b \to 0$, so that (4.14) is satisfied exactly in the limit, whereas (4.15) is not even qualitatively valid. [The approximation (4.15) is certainly not new, but we have been unable to find any systematic investigation of its accuracy.]

We give alternative approximations to A_1 and M, in §6 below, that are exact to second order in ϵ if $\eta(x)$ is continuous over the closed interval of the obstacle. These approximations, which also are exact for a semi-ellipse, are compared with those of (4.14) and (4.15) for a finite, asymmetric obstacle in §7 and for an infinite obstacle in §8. The latter comparison implies that (4.14) and (4.15) are not satisfactory for infinite obstacles.

5. Low-speed limit ($k \to \infty$)

We now construct a singular integral equation for $f(x)$ in the limit $k \to \infty$ with κ fixed and reduce its solution to the solution of the Dirichlet problem (of potential theory) for a half-plane.

We begin with the following definitions: (i) $\mathscr{C}$ is a class of functions of the real variable x that are continuous and belong to $L^2(-\infty,\infty)$. (ii) $\mathbf{C}$ is a class of functions of the complex variable $\mathbf{x} = x + ix_i$ that are holomorphic in the half-plane $x_i > 0$ and $O(1/|\mathbf{x}|)$ as $|\mathbf{x}| \to \infty$ in $x_i > 0$. (iii) The Hilbert transform (Titchmarsh 1948, chapter 5) of $f(x)$ is given by

$$f_*(x) \equiv \frac{1}{\pi} \fint_{-\infty}^{\infty} \frac{f(\xi)\,d\xi}{\xi - x} \quad (f \text{ in } \mathscr{C}), \tag{5.1}$$

where the Cauchy principal value of the integral is implied by the crossed integral sign; $f_*(x)$ is in $\mathscr{C}$ if $f(x)$ is in $\mathscr{C}$. (iv) The Cauchy integral of $f(x)$, given by

$$\mathbf{f}(\mathbf{x}) = \frac{1}{\pi i} \int_{-\infty}^{\infty} \frac{f(\xi)\,d\xi}{\xi - \mathbf{x}} \quad (x_i > 0), \tag{5.2}$$

is in $\mathbf{C}$ and reduces to

$$\mathbf{f}(\mathbf{x}) = f(x) - i f_*(x) \quad (x_i = 0+) \tag{5.3}$$

on the real axis. Accordingly, $\mathbf{f}(\mathbf{x})$ is a solution to the Dirichlet problem for prescribed $f(x)$ in $\mathscr{C}$ [the most general solution is $\mathbf{f}+iC$, where C is a real constant that vanishes identically in the present context; see Titchmarsh (1948, chapter 5) and Muskhelishvili (1953, chapter 2) for more general discussions].

Turning to the construction of the integral equation for $f(x)$, we replace x by $\mathbf{x}$ in (2.2), let $k\to\infty$ and $x_i\to 0+$ while holding x and y fixed, and integrate by parts with respect to α to obtain the asymptotic approximation

$$\delta_1(x,y) \sim \mathscr{R}\{i\mathbf{x}^{-1}\exp(iky)\}+O(k^{-1}) \quad (k\to\infty,\ x_i\to 0+). \tag{5.4}$$

Substituting (5.4) into (2.1*a*) and invoking (5.2) and (5.3) on the hypothesis that $f(x)$ is in $\mathscr{C}$, we obtain

$$\delta(x,y) \sim \mathscr{R}\{\exp(iky)\mathbf{f}(\mathbf{x})\} \quad (x_i\to 0+) \tag{5.5a}$$

$$= f(x)\cos ky + f_*(x)\sin ky, \tag{5.5b}$$

where, here and subsequently, the asymptotic limit $k\to\infty$ is implicit, and the error is $O(1/k)$ relative to unity. Invoking the boundary condition (1.4), we set $y/\epsilon = \delta = \eta$ and $k = \kappa/\epsilon$ in (5.5*b*) to obtain the singular integral equation

$$\eta(x) = f(x)\cos\{\kappa\eta(x)\} + \frac{\sin\{\kappa\eta(x)\}}{\pi}\,⨍_{-\infty}^{\infty}\frac{f(\xi)\,d\xi}{\xi - x}. \tag{5.6}$$

Muskhelishvili (1953, §47) gives a solution of an integral equation that is equivalent to (5.6), but we find it rather more economical to proceed independently. Multiplying (5.6) through by $\exp(\kappa\eta_*)$ and invoking the definition (5.3) for $\boldsymbol{\eta}$, we obtain

$$g(x) \equiv \eta\exp(\kappa\eta_*) = \mathscr{R}\{\exp(i\kappa\boldsymbol{\eta})\mathbf{f}\} \quad (x_i = 0+). \tag{5.7}$$

Now, by hypothesis, both η and f are in $\mathscr{C}$, in virtue of which g also is in $\mathscr{C}$ and each of $\boldsymbol{\eta}$,

$$\mathbf{g}(\mathbf{x}) = \exp[i\kappa\boldsymbol{\eta}(x)]\mathbf{f}(\mathbf{x}), \tag{5.8}$$

and

$$\mathbf{f}(\mathbf{x}) = \exp[-i\kappa\boldsymbol{\eta}(\mathbf{x})]\mathbf{g}(\mathbf{x}) \tag{5.9}$$

is in C. Letting $x_i\to 0+$ in (5.9) and invoking (5.3) and (5.7), we obtain

$$f - if_* = (g - ig_*)\exp[-\kappa(\eta_* + i\eta)] \tag{5.10}$$

or, equivalently,

$$f = \eta\cos\kappa\eta + \zeta\sin\kappa\eta \tag{5.11a}$$

and

$$f_* = \eta\sin\kappa\eta - \zeta\cos\kappa\eta, \tag{5.11b}$$

where

$$\zeta(x) \equiv -\exp[-\kappa\eta_*(x)]g_*(x) \tag{5.12a}$$

$$= \frac{1}{\pi}⨍_{-\infty}^{\infty}\frac{\eta(\xi)\,d\xi}{(x-\xi)}\exp\left\{\frac{-\kappa(x-\xi)}{\pi}⨍_{-\infty}^{\infty}\frac{\eta(\lambda)\,d\lambda}{(x-\lambda)(\xi-\lambda)}\right\}. \tag{5.12b}$$

We remark that (5.11*a*) yields the correct solution in the limit $\kappa\to 0$, namely $f(x)\to\eta(x)$.

Substituting (5.9) into (5.5*a*) or, equivalently, (5.11*a, b*) into (5.5*b*), we obtain

$$\delta(x,y) \sim \mathscr{R}\{\exp[i(ky - \kappa\boldsymbol{\eta})]\mathbf{g}\} \quad (x_i = 0+) \tag{5.13a}$$

$$= \eta\cos\{k(y-\epsilon\eta)\} - \zeta\sin\{k(y-\epsilon\eta)\} \tag{5.13b}$$

$$= (\eta^2+\zeta^2)^{\frac{1}{2}}\cos\{k(y-\epsilon\eta)+\tan^{-1}(\zeta/\eta)\} \tag{5.13c}$$

as alternative, asymptotic representations of $\delta(x, y)$ in the limit $k \to \infty$ with x and ky fixed. We may obtain representations that are, respectively, valid as $r \to \infty$ or uniformly valid with respect to r by substituting $f(x)$ from (5.11 *a*) into (2.9 *a*) or (2.1 *a*).

Differentiating (5.13 *c*) with respect to y, we obtain

$$(\epsilon\delta_y)_{\max} = [\kappa\{\eta^2(x) + \zeta^2(x)\}^{\frac{1}{2}}]_{\max}, \tag{5.14}$$

from which we infer that the stability criterion (1.6) is violated for sufficiently large κ, say $\kappa > \kappa_c$. Indeed, since

$$(\eta^2 + \zeta^2)^{\frac{1}{2}}_{\max} \geqslant \eta_{\max} \equiv 1, \tag{5.15}$$

we infer that $\kappa_c < 1$ for a slender obstacle. This suggests that $\zeta(x)$ and $f(x)$ may be expanded in powers of κ within the range of physical interest.

Turning to the calculation of the scattering cross section and drag, we invoke the identity (essentially an analogue of the well-known Dirichlet integral)

$$\lim_{k\to\infty} x^{-1} J_1(kx) = 2\hat{\delta}(x) \tag{5.16}$$

in (3.7) to obtain

$$Q \sim 2\kappa^2 b \int_{-\infty}^{\infty} f^2(x)\,dx \tag{5.17a}$$

$$= 2\kappa^2 b \int_{-\infty}^{\infty} (\eta\cos\kappa\eta + \zeta\sin\kappa\eta)^2\,dx, \tag{5.17b}$$

where (5.17 *b*) follows from (5.17 *a*) by virtue of (5.11 *a*).

Invoking the fact that $\mathbf{H}_1(x)$ is a bounded function of x that tends uniformly to $2/\pi$ as $x \to \infty$, we reduce (3.8) to

$$C_D \sim (2\kappa/\pi) \int_{-\infty}^{\infty} \fint_{-\infty}^{\infty} f(x) f'(\xi)(x-\xi)^{-1}\,d\xi\,dx \tag{5.18a}$$

$$= 2\kappa \int_{-\infty}^{\infty} f'(x) f_*(x)\,dx \tag{5.18b}$$

$$= (2\kappa/\pi) \int_{-\infty}^{\infty} \int_{-\infty}^{\infty} f'(x) f'(\xi) \log|x-\xi|^{-1}\,d\xi\,dx, \tag{5.18c}$$

where (5.18 *b*) follows from (5.18 *a*) by virtue of (5.1) and (5.18 *c*) follows from (5.18 *a*) by integration by parts. [It can be shown that the error in passing from (3.8) to (5.18 *a*) is $O(1/k)$ relative to unity.] The aerodynamicist will not miss the correspndence between (5.18 *c*) and both Prandtl's result for (the lifting-line approximation to) the vortex drag of a finite-wing in an incompressible flow and von Kármán's result for the wave drag on a pointed, slender body of revolution in supersonic flow (Ward 1955, p. 204).

Substituting (5.11 *a*, *b*) into (5.18 *b*), eliminating $\zeta'(x)$ from the integrand by integration by parts, and remarking that

$$\int_{-\infty}^{\infty} (\eta\cos\kappa\eta)'\eta\sin\kappa\eta\,dx = 0 \tag{5.19}$$

by virtue of the fact that η vanishes at the end-points of the integration, we reduce the result to

$$C_D = -\kappa \int_{-\infty}^{\infty} \{2\zeta(x) + \kappa\zeta^2(x)\}\eta'(x)\,dx. \tag{5.20}$$

We notice that this result is not generally invariant under a reversal of the flow (see last paragraph in §3 above).

We obtain a composite approximation to the lee-wave spectrum that is valid for all k as $\epsilon \to 0$, for all ϵ as $k \to 0$, and for fixed κ as $k \to \infty$ by the simple expedient of multiplying the Fourier transform of (5.11*a*) by $1 + (M/A)$. It would appear to be adequate for this approximation to expand (5.11*a*) and (5.12*b*) in κ to obtain

$$F(\alpha) = \pi^{-1}\{1 + (M/A)\} \int_{-\infty}^{\infty} \exp(-i\alpha x)\eta(x) \Big[1 - \kappa\eta_*(x) - \tfrac{1}{2}\kappa^2\eta^2(x) - (\kappa^2/\pi)\int_{-\infty}^{\infty} (x-\xi)^{-1}\{\eta_*(x) - \eta_*(\xi)\}\eta(\xi)\,d\xi + O(\kappa^3)\Big]\,dx \quad (\alpha < k). \tag{5.21}$$

We add that (5.21) is valid for all α if $\epsilon \ll 1$ ($M/A \to 0$); however, the calculation of the lee-wave field and drag require $F(\alpha)$ only in $\alpha < k$.

6. Second-order approximation

Invoking (1.4) in (2.1*a*), we obtain the integral equation

$$\eta(x) = \pi^{-1} \int_{-\infty}^{\infty} f(\xi)\,\delta_1\{x-\xi,\ \epsilon\eta(x)\}\,d\xi \tag{6.1}$$

for $f(x)$. We have already established that the perturbation field of the obstacle is given to first order in ϵ by the planar approximation (2.5). We now determine a second-order approximation to this field, approximating the kernel in (6.1) by

$$\delta_1\{x-\xi,\ \epsilon\eta(x)\} = \delta_1(x-\xi,\ 0+) + \epsilon\{\partial\delta_1(x-\xi,\ y)/\partial y\}_{y=0+}\,\eta(x) + O(\epsilon^2) \tag{6.2}$$

on the hypothesis that the resulting integral over ξ converges (see below). Substituting (6.2) into (6.1), invoking (2.4*b*) and introducing

$$g_1(x) = -\pi^{-1}\{\partial\delta_1(x,y)/\partial y\}_{y=0+} \tag{6.3a}$$

$$= \frac{1}{\pi} \lim_{y\to 0+} \mathscr{R} \int_0^{\infty} (\alpha^2 - k^2)^{\frac{1}{2}} \exp\{i\alpha x - (\alpha^2 - k^2)^{\frac{1}{2}} y\}\,d\alpha, \tag{6.3b}$$

we obtain

$$\eta(x) = f(x) - \epsilon\eta(x) \int_{-\infty}^{\infty} g_1(x-\xi) f(\xi)\,d\xi \tag{6.4a}$$

$$= f(x) - \epsilon\eta(x)\mathscr{R} \int_0^{\infty} (\alpha^2 - k^2)^{\frac{1}{2}} F(\alpha) \exp(i\alpha x)\,d\alpha, \tag{6.4b}$$

where $F(\alpha)$ is the Fourier transform of $f(x)$, as defined by (2.3). Replacing $f(\xi)$ by its first approximation, $\eta(\xi)$, in (6.4*a*) and designating the corresponding first approximation to $F(\alpha)$ by

$$F^{(1)}(\alpha) = \pi^{-1} \int_{-\infty}^{\infty} \eta(\xi) \exp(-i\alpha\xi)\,d\xi \tag{6.5}$$

in (6.4*b*), we obtain the second approximation to $f(x)$ in the alternative forms

$$f^{(2)}(x) = \eta(x)\left\{1+\epsilon\int_{-\infty}^{\infty} g_1(x-\xi)\,\eta(\xi)\,d\xi\right\} \tag{6.6a}$$

$$= \eta(x)\left\{1+\epsilon\mathscr{R}\int_0^{\infty}(\alpha^2-k^2)^{\frac{1}{2}}F^{(1)}(\alpha)\exp{(i\alpha x)}\,d\alpha\right\}. \tag{6.6b}$$

Replacing α by β in (6.6*b*) and then taking the Fourier transform of $f^{(2)}(x)$ in accordance with (2.3*a*), we obtain

$$F^{(2)}(\alpha) = F^{(1)}(\alpha)+\tfrac{1}{2}\epsilon\int_{-\infty}^{\infty}F^{(1)}(\alpha-\beta)\,F^{(1)}(\beta)\,(\beta^2-k^2)^{\frac{1}{2}}\,d\beta, \tag{6.7}$$

where
$$(\beta^2-k^2)^{\frac{1}{2}} = -i(k^2-\beta^2)^{\frac{1}{2}}\operatorname{sgn}\beta \quad (|\beta|<k). \tag{6.8}$$

The approximation (6.6) is not uniformly valid in the neighbourhood of a stagnation point but suffices for the first-order approximations, within error factors of $1+O(\epsilon^2)$, to the lee-wave field and wave drag for an obstacle that is not more blunt than a semi-ellipse. It breaks down completely for an obstacle for which $\eta(x)$ is discontinuous; e.g. $f(x)-\eta(x)$ is $O(\epsilon\log\epsilon)$, rather than $O(\epsilon)$, for a rectangular obstacle. Uniformly valid solutions may be obtained with the aid of the techniques discussed by Van Dyke (1964).

We obtain the limiting form of the integral in (6.6*a*) by substituting g_1 from (6.3*b*), setting $k=0$, integrating by parts with respect to ξ, invoking the requirement that $\eta(\xi)$ vanish at the end points, carrying out the α-integration, letting $y\to 0+$ and invoking (5.1):

$$\begin{aligned}\lim_{k\to 0}\int_{-\infty}^{\infty} g_1(x-\xi)\,\eta(\xi)\,d\xi &= \frac{1}{\pi}\lim_{y\to 0+}\int_{-\infty}^{\infty}\eta(\xi)\,d\xi\int_0^{\infty}\alpha\exp{(-\alpha y)}\cos{\{\alpha(x-\xi)\}}\,d\alpha\\ &= \frac{1}{\pi}\lim_{y\to 0+}\int_{-\infty}^{\infty}\eta'(\xi)\,d\xi\int_0^{\infty}\exp{(-\alpha y)}\sin{\{\alpha(x-\xi)\}}\,d\alpha\\ &= \frac{1}{\pi}\,⨍_{-\infty}^{\infty}\frac{\eta'(\xi)\,d\xi}{x-\xi} = -\eta_*'(x),\end{aligned}$$

in virtue of which
$$f^{(2)}(x)\to\eta(x)\{1-\epsilon\eta_*'(x)\}\quad (k\to 0). \tag{6.9}$$

Carrying out a more elaborate investigation, we find that the error term in (6.9) is typically $O(k^2,\,\epsilon k^2\log k)$, although it may be $O(k)$ if $\eta(x)$ does not vanish either identically or exponentially as $|x|\to\infty$, as in the example of the Witch of Agnesi (see §8 below).

We obtain alternative representations of the second-order approximation to the dipole form either by setting $\alpha=k=0$ in (6.7) or by substituting (6.9) into (4.6) to obtain F_0 and then invoking (4.7) and $F_0^{(1)}\equiv A/\pi bh$:

$$A_1 = \pi^{-1}A+h^2\int_0^{\infty}|F^{(1)}(\beta)|^2\beta\,d\beta \tag{6.10a}$$

$$= \pi^{-1}\left\{A-h^2\int_{-\infty}^{\infty}\eta(x)\eta_*'(x)\,dx\right\}. \tag{6.10b}$$

Comparing (6.10a,b) to (4.12), we obtain

$$M = \pi h^2 \int_0^\infty |F^{(1)}(\beta)|^2 \beta\, d\beta \tag{6.11a}$$

$$= -\int_{-\infty}^{\infty} h(x)\, h'_*(x)\, dx \quad [h(x) \equiv h\eta(x)] \tag{6.11b}$$

as the corresponding approximations to the virtual mass. Introducing the Fourier-series representation

$$h\eta(x) = \sum_1^\infty h_n \sin n\theta, \quad x = \cos\theta \tag{6.12}$$

for an obstacle of finite base, we obtain

$$M = \tfrac{1}{2}\pi \sum_1^\infty n h_n^2 \tag{6.13}$$

and

$$A_1 = \tfrac{1}{2} b h_1 + \frac{1}{2} \sum_1^\infty n h_n^2. \tag{6.14}$$

We remark that these last results also may be obtained by expanding the mapping of $C + C_*$ on the unit circle in powers of ϵ and invoking Pölya's (1947) results for M and A_1 in terms of this mapping.

Turning to the limit $k \to \infty$, we substitute (5.4) into (6.3a) to obtain the required approximation to g_1 and substitute the result into (6.6a) to obtain

$$f(x) = \eta(x)\{1 - \kappa \eta_*(x)\} \quad (k \to \infty), \tag{6.15}$$

as otherwise may be inferred from (5.11a) and (5.13) within the same approximation.

7. Semi-elliptical obstacle

As a first example, we consider a semi-elliptical obstacle of base $2b$ and height h, for which

$$\eta(x) = (1 - x^2)^{\frac{1}{2}} H(1 - |x|) \tag{7.1}$$

and, from (6.5),

$$F^{(1)}(\alpha) = \alpha^{-1} J_1(\alpha). \tag{7.2}$$

The results are summarized and compared with those for the obstacles treated subsequently in table 2.

Substituting (7.2) into (3.3b), expanding $J_1^2(\alpha)$ in a power series, and integrating term by term, we obtain the first-order approximation

$$C_{D1} = \pi\epsilon \sum_{n=0}^\infty \frac{(-)^n k^{2n+3}}{(n+1)!\,(n+2)!\,(2n+3)} \quad (\epsilon \to 0). \tag{7.3}$$

Remarking that

$$\frac{1}{\pi\epsilon} \frac{dC_{D1}}{dk} = \sum_{n=0}^\infty \frac{(-)^n k^{2n+2}}{(n+1)!\,(n+2)!} \tag{7.4a}$$

$$= 1 - k^{-1} J_1(2k) \tag{7.4b}$$

$$= 1 + 2J_1'(2k) - 2J_0(2k), \tag{7.4c}$$

we obtain

$$C_{D1} = \pi\epsilon \left\{ k + J_1(2k) - \int_0^{2k} J_0(x)\, dx \right\} \quad (\epsilon \to 0), \tag{7.5}$$

Obstacle	$\eta(x)$	A	$F^{(1)}(\alpha)$	C_D/k^3 $(\epsilon \to 0)$	$C_D/\pi\kappa$ $(k \to \infty)$	κ_c
Semi-ellipse 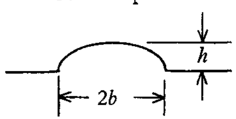	$\sqrt{(1-x^2)}$ $(\lvert x\rvert < 1)$	$\frac{1}{2}\pi bh$	$\dfrac{J_1(\alpha)}{\alpha}$	$\frac{1}{6}\pi(1+\epsilon)^2 \times (1-\frac{1}{10}k^2+\ldots)$	$1+\frac{3}{4}\kappa^2+\ldots$	0·67
Generalized ellipse 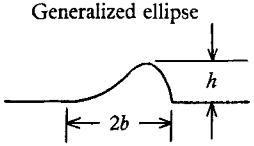	$\dfrac{4}{3\sqrt{3}}(1\pm x)\sqrt{(1-x^2)}$ $(\lvert x\rvert < 1)$	$\dfrac{2\pi bh}{3\sqrt{3}}$	$\dfrac{4}{3\sqrt{3}}\left\{\dfrac{J_1(\alpha)\mp iJ_2(\alpha)}{\alpha}\right\}$	$\frac{8}{81}(1+\frac{8}{9}\epsilon)^2 \times (1-\frac{3}{40}k^2+\ldots)$	$\dfrac{8}{9}\left(1\pm\dfrac{8\kappa}{9\sqrt{3}} + \frac{7}{9}\kappa^2+\ldots\right)$	0·82 0·58
Witch of Agnesi 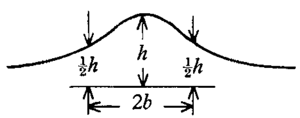	$\dfrac{1}{1+x^2}$	πbh	$\exp(-\lvert\alpha\rvert)$	$\frac{2}{3}\pi(1+\frac{1}{4}\epsilon)^2\left(1-\dfrac{3\pi}{8}k+\ldots\right)$	$\frac{1}{2}(1+\frac{7}{16}\kappa^2+\ldots)$	0·85
Rectangle 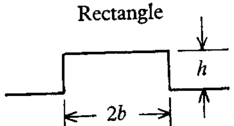	$1\ (\lvert x\rvert < 1)$	$2bh$	$\dfrac{2\sin\alpha}{\pi\alpha}$	$\dfrac{8}{3\pi}\left\{1+\dfrac{2\epsilon}{\pi}\left(\log\dfrac{4\pi}{\epsilon}+\frac{1}{2}\right)\right\}^2 \times (1-\frac{2}{15}k^2+\ldots$	$\dfrac{4}{\pi^2}(\log 4k+\gamma-1)$	0

TABLE 2. The principal properties of the obstacles considered in §§7–9.

which contains only tabulated functions and yields the asymptotic approximation†

$$C_{D1} \sim \pi\kappa\{1-k^{-1}+O(k^{-\frac{5}{2}})\} \quad (\epsilon \to 0,\ k \to \infty). \tag{7.6}$$

The results for $C_{D1}/(\frac{1}{6}\pi\epsilon k^3)$ and $C_{D1}/\pi\kappa$, which tend to unity as $k \to 0$ and $k \to \infty$, respectively, are plotted in figures 2 and 3.

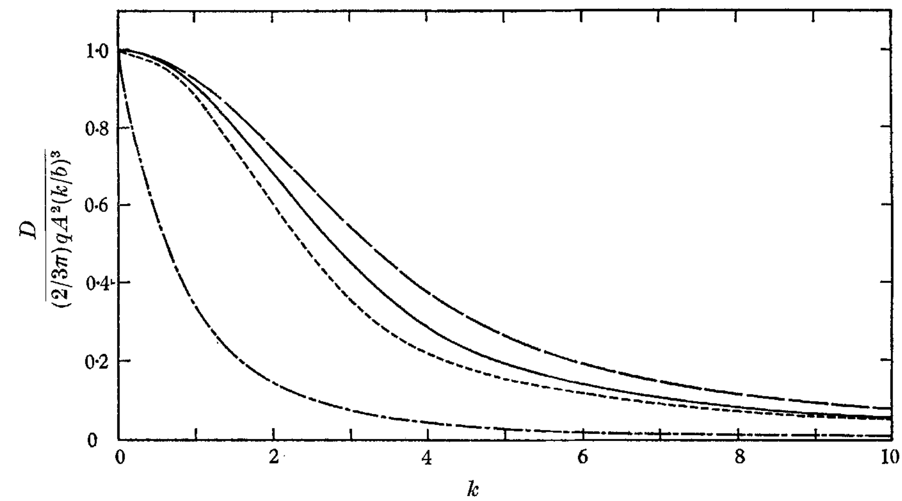

FIGURE 2. The first-order approximation to the wave drag, relative to the limiting value as $k \to 0$. — —, generalized ellipse ($a = 1$); ——, ellipse; - - -, rectangle; — - —, Witch of Agnesi.

Substituting (4.14) into (4.8), we obtain

$$C_D \to \tfrac{1}{6}\pi\epsilon k^3(1+\epsilon)^2 \quad (k \to 0), \tag{7.7}$$

which reduces to the leading term in (7.3) as $\epsilon \to 0$.

The Hilbert transform of (7.1), as defined in (5.1), is given by

$$\eta_*(x) = -x+(x^2-1)^{\frac{1}{2}}H(|x|-1)\operatorname{sgn} x. \tag{7.8}$$

Substituting (7.8) into (5.12*b*), we obtain

$$\zeta(x) = \frac{\exp(\kappa x)}{\pi} \int_{-1}^{1} \frac{\exp(-\kappa\xi)(1-\xi^2)^{\frac{1}{2}}\,d\xi}{x-\xi} \quad (|x| < 1) \tag{7.9a}$$

$$= x + \int_0^{\kappa} \exp(\lambda x) I_1(\lambda)\lambda^{-1}\,d\lambda \tag{7.9b}$$

$$= x + \tfrac{1}{2}\kappa + \tfrac{1}{4}\kappa^2 x + \tfrac{1}{12}\kappa^3(\tfrac{1}{4}+x^2) + O(\kappa^4), \tag{7.9c}$$

where the identity between (7.9*a*) and (7.9*b*) may be established by introducing the integral representation of the modified Bessel function I_1 and reversing the order of integration. Carrying out the corresponding calculation for $|x| > 1$, we find that the maximum value of ζ occurs at $x = 1$. Substituting (7.9*c*) into

† We infer from the aforementioned analogy with Prandtl's lifting-line theory [see remark following (5.18*c*)] and (7.6) that the minimum drag for an obstacle of prescribed breadth and area in the joint limit $\epsilon \to 0$, $k \to \infty$ is $D = \pi\kappa q h$.

(5.14), we find that the maximum value of $\eta^2+\zeta^2$ also occurs at $x = 1$ and that $\kappa_c = 0{\cdot}67$; accordingly, (7.9*c*) provides an adequate approximation within the range of physical interest. Substituting (7.1) and (7.9*c*) into (5.11*a*) and (5.20), we obtain

$$f(x) = (1-x^2)^{\frac{1}{2}}\{1+\kappa x+\tfrac{1}{2}\kappa^2x^2+\tfrac{1}{6}\kappa^3x(\tfrac{1}{2}+x^2)+O(\kappa^4)\} \quad (7.10)$$

and

$$C_D \sim \pi\kappa\{1+\tfrac{3}{4}\kappa^2+O(\kappa^4, k^{-1})\} \quad (k\to\infty). \quad (7.11)$$

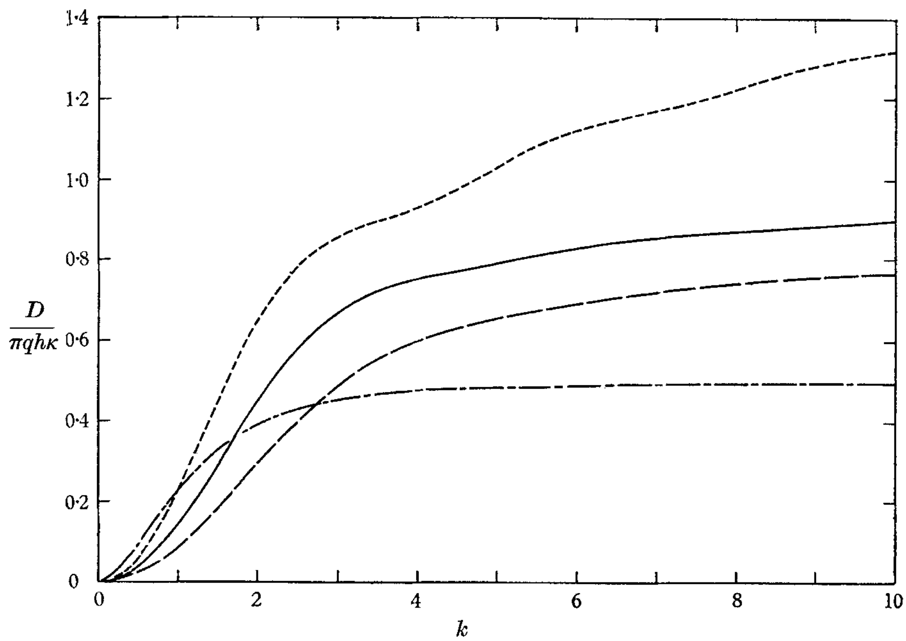

FIGURE 3. The first-order approximation to the wave-drag, relative to the limiting value for a semi-elliptical obstacle as $k\to\infty$. – – –, rectangle; ——, ellipse; — —, generalized ellipse ($a = 1$); — · —, Witch of Agnesi.

A numerical integration of (5.20), in conjunction with (7.9*b*), reveals that the first and second approximations provided by (7.11) are accurate to within 28 and 3.5 %, respectively, for $0 < \kappa < 0{\cdot}67$.

Substituting $M/A = \epsilon$, (7.1), and (7.8) into (5.21), we obtain (after some manipulation)

$$F(\alpha) = (1+\epsilon)\alpha^{-1}\{J_1 - i\kappa J_2+\tfrac{1}{2}\kappa^2(J_1-3\alpha^{-1}J_2)+iC\kappa^3+O(\kappa^4)\} \quad (\alpha < k), \quad (7.12)$$

where C is a real constant. Substituting (7.12) into (3.3*b*) and proceeding as in (7.3)–(7.5), we obtain the composite approximation

$$C_D = (1+\epsilon)^2[(1+2\kappa^2)C_{D1}+\pi\kappa^3\{k^{-2}J_2(2k)-\tfrac{3}{2}k^{-3}J_1(2k)+\tfrac{3}{2}k^{-2}-\tfrac{5}{4}\}] \quad (7.13a)$$

$$= (1+\epsilon)^2C_{D1} \quad (\kappa\to 0), \quad (7.13b)$$

where C_{D1} is given by (7.5). The approximation (7.13*a*) is compared with the approximations of (7.5), the aforementioned numerical integration of (5.18), and the solution obtained in III in figures 4*a*, *b*.

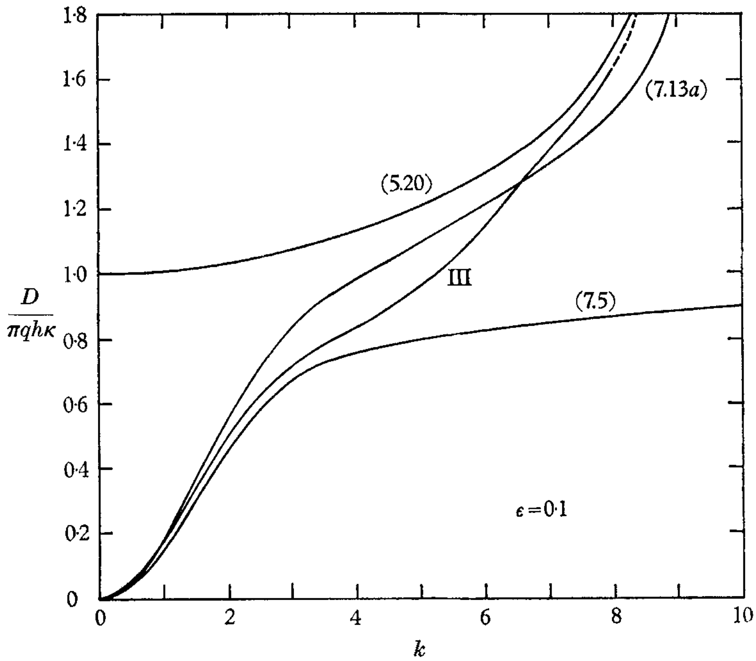

FIGURE 4a. The wave drag on a slender semi-elliptical obstacle as given by the first-order approximation of (7.5), the asymptotic approximation of (5.20), the composite approximation of (7.13a) and the reference solution of III, all for $\epsilon = 0{\cdot}1$.

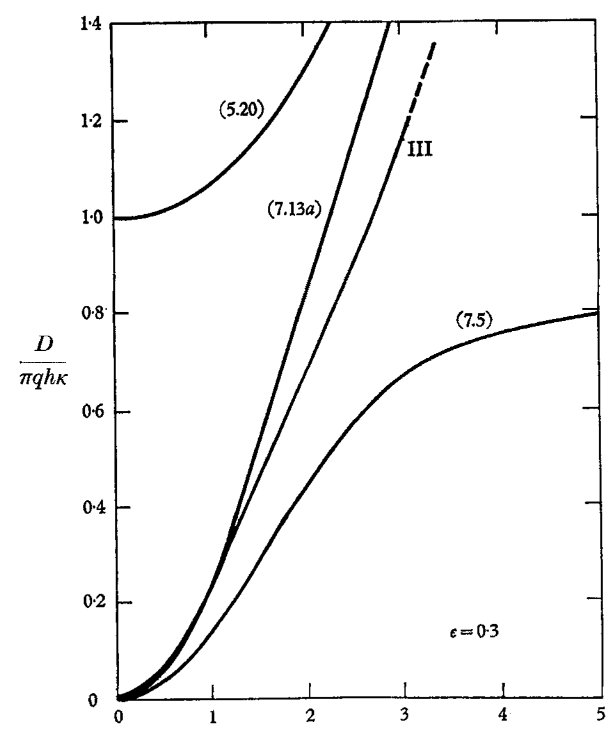

FIGURE 4b. The wave drag on a slender semi-elliptical obstacle as given by the first-order approximation of (7.5), the asymptotic approximation of (5.20), the composite approximation of (7.13a) and the reference solution of III, all for $\epsilon = 0{\cdot}3$.

We give only the limiting approximations to the total scattering cross section, as obtained from (4.7) and (5.16a):

$$Q \to \tfrac{1}{8}\pi^2\epsilon^2(1+\epsilon)^2k^3b \quad (k\to 0) \tag{7.13c}$$

and

$$Q \sim \tfrac{8}{3}\kappa^2 b\{1+\tfrac{2}{5}\kappa^2+O(\kappa^4, k^{-1})\} \quad (k\to\infty). \tag{7.14}$$

Generalized ellipse

We illustrate the effects of asymmetry by generalizing (7.1) to obtain the family

$$\eta(x) = \eta_0(1+ax)(1-x^2)^{\frac{1}{2}}H(1-|x|) \quad (|a| \leqslant 1), \tag{7.15}$$

where η_0 and a are implicitly related by the requirement that (from the definition of ϵ) $\max\{\eta(x)\} = 1$. Invoking (6.5), we obtain

$$F^{(1)}(\alpha) = \eta_0\alpha^{-1}\{J_1(\alpha)-iaJ_2(\alpha)\}. \tag{7.16}$$

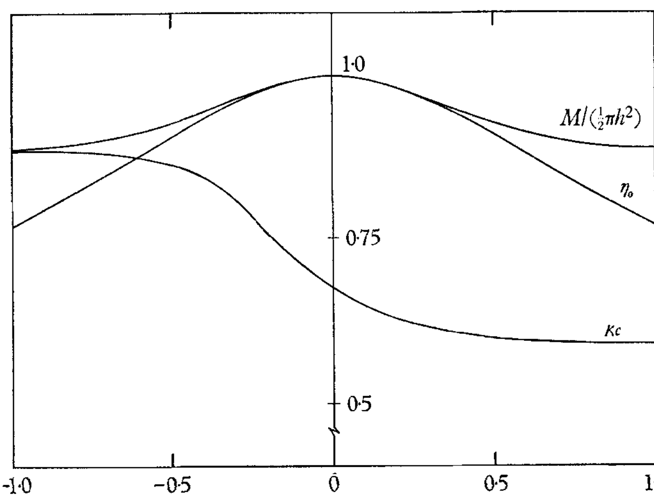

FIGURE 5. The area parameter η_0, the virtual-mass parameter $(1+\frac{1}{2}a^2)\eta_0^2$, and κ_c for the generalized ellipse.

Substituting (7.16) into (3.3b) and proceeding as in (7.3)–(7.5), we obtain the first-order approximation

$$C_{D1} = \pi\epsilon\eta_0^2\left[(1+\tfrac{1}{2}a^2)k+(1+a^2)\left\{J_1(2k)-\int_0^{2k}J_0(x)\,dx\right\}+a^2k^{-1}J_2(k)\right], \tag{7.17a}$$

$$\sim \pi\kappa\eta_0^2\{1+\tfrac{1}{2}a^2-(1+a^2)k^{-1}+O(k^{-\frac{3}{2}})\} \quad (k\to\infty). \tag{7.17b}$$

The result (7.17a) is plotted in figure 6.

The Hilbert transform of (7.15) is

$$\eta_*(x) = \eta_0[\tfrac{1}{2}a+(1+ax)\{-x+(x^2-1)^{\frac{1}{2}}H(|x|-1)\operatorname{sgn}x\}]. \tag{7.18}$$

Substituting (7.18) into (6.10b) and (6.11b), we obtain

$$A_1 = \tfrac{1}{2}\eta_0 hb\{1+\epsilon(1+\tfrac{1}{2}a^2)\eta_0\} \tag{7.19}$$

and

$$M = \tfrac{1}{2}\pi h^2\eta_0^2(1+\tfrac{1}{2}a^2). \tag{7.20}$$

The area and virtual-mass parameters, η_0 and $(1+\frac{1}{2}a^2)\eta_0^2$, are plotted in figure 5. The maximum deviation of the latter parameter from unity is 11 %, which provides additional support for the simple approximation of (4.15).

Substituting (7.15) and (7.18) into (5.12*b*), we obtain a double integral for $\zeta(x)$; substituting $\zeta(x)$ into (5.14), and carrying out a numerical evaluation, we obtain the values of κ_c plotted in figure 5. Calculating $\zeta(x)$ through $O(\kappa^2)$ and substituting the result into (5.20), we obtain

$$C_D = \pi\kappa\eta_0^2\{1+\tfrac{1}{2}a^2+a\eta_0\kappa+\tfrac{3}{4}(1+\tfrac{3}{2}a^2+\tfrac{1}{8}a^4)\eta_0^2\kappa^2+O(\kappa^3,k^{-1})\} \quad (k\to\infty). \quad (7.21)$$

We infer from (7.21) that the drag is not invariant under a reversal of the flow for $k \gg 1$ and that the drag of the obstacle with a cusped leading edge and blunt trailing edge ($a > 0$) is larger than the drag on the reversed obstacle ($a \to -a$).

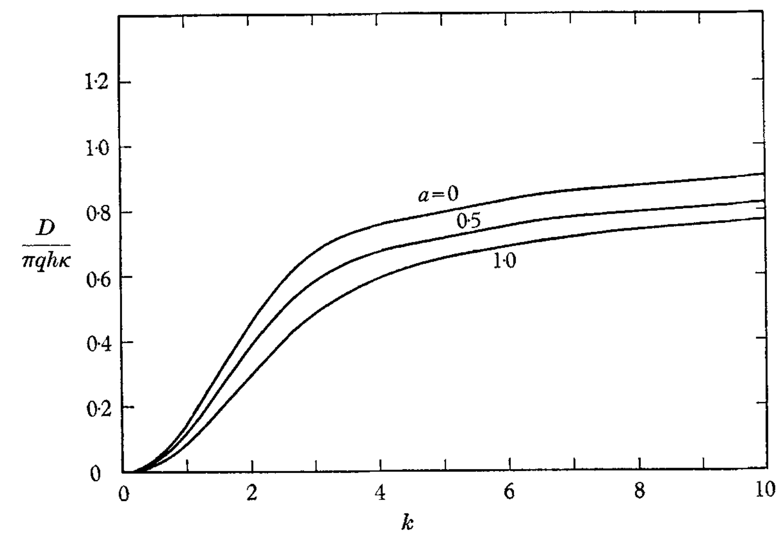

FIGURE 6. The wave drag on a generalized ellipse, as given by (7.17).

8. Witch of Agnesi

The infinite obstacle described by

$$\eta(x) = (1+x^2)^{-1} \quad (8.1)$$

and known as the *Witch of Agnesi*† in the special case $\epsilon = 1$, was considered originally by Queney (1948; see also Yih 1965, pp. 68–71) in the context of a uniform flow in an isothermal atmosphere; however, he did not calculate the drag. Its Fourier transform, as defined by (6.5), is

$$F^{(1)}(\alpha) = \exp(-|\alpha|), \quad (8.2)$$

which provides an especially simple basis for the second-order calculation of §6.

† The curve described by (8.1) appears to have been studied originally by both Fermat and Grandi (Archibald & Court 1964). Grandi designated it both *versiora* (because the curvature takes *opposite* signs) and, in a letter to Galileo (1718, p. 393), *Versiera*. Maria Agnesi studied it in her *Instituzioni Analitiche* (1748; see Colson 1801) and also designated it *Versiera*, a term that evidently has no direct translation but is similar to the Italian word *avversoria*, which has the first and second meanings *adversary* and *devil*. The Reverend John Colson (1801) appears to have opted for a feminine equivalent of the latter meaning and designated the curve *Witch of Agnesi*, by which name it is still known.

Substituting (8.2) into (3.3*b*), we obtain

$$C_{D1} = 2\pi\epsilon k^3\int_0^1 \exp(-2kt)(1-t^2)^{\frac{1}{2}}t\,dt \quad (\epsilon\to 0) \tag{8.3a}$$

$$= \tfrac{2}{3}\pi\epsilon k^3[1+\tfrac{3}{4}\pi k^{-1}\{\mathbf{L}_2(2k)-I_2(2k)\}] \tag{8.3b}$$

$$= \tfrac{2}{3}\pi\epsilon k^3\left\{1-\frac{3\pi}{8}k+\tfrac{4}{5}k^2+\dots\right\} \tag{8.3c}$$

$$\sim \tfrac{1}{2}\pi\kappa\{1-\tfrac{3}{4}k^{-2}+O(k^4)\} \quad (\epsilon\to 0, k\to\infty), \tag{8.3d}$$

where $\mathbf{L}_2$ is a modified Struve function.

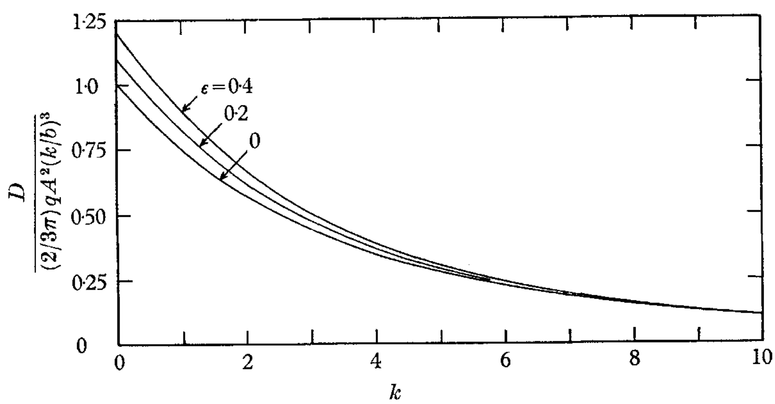

FIGURE 7. The first- and second-order approximations to the wave drag on the Witch of Agnesi.

We remark that $C_{D1}/\epsilon k^3$ contain odd, as well as even, powers of k, despite the fact that η is even in x. This is in contrast to the other configurations considered here and reflects the fact that $\eta(x)$ decays only algebraically as $|x|\to\infty$. We also remark that the limiting drag as $k\to\infty$ and $\epsilon\to 0$ is half the corresponding drag on a semi-elliptical obstacle of the same *height* (referring to the footnote in §7, we recall that the latter drag is the minimum possible for prescribed breadth and area). The result (8.3*a*) was obtained by Sawyer (1959) and evaluated numerically at $k = 1$ and $k = \infty$. The result (8.3*b*) is plotted in figures 2 and 3.

Substituting (8.1) into (6.10*a*) and (6.11*a*), we obtain the second-order approximations

$$A_1 = bh(1+\tfrac{1}{4}\epsilon) \tag{8.4}$$

and

$$M = \tfrac{1}{4}\pi h^2. \tag{8.5}$$

The latter result differs from the simpler approximation (4.15) by a factor of two, which suggests the inadequacy of that approximation for infinite obstacles.

The Hilbert transform of (8.1) is

$$\eta_*(x) = -x(1+x^2)^{-1}. \tag{8.6}$$

Substituting (8.1) and (8.6) into (5.12*b*), calculating $\zeta(x)$, and substituting the result into (5.14) and (5.20), we obtain $\kappa_c = 0·85$ and

$$C_D \sim \tfrac{1}{2}\pi\kappa\{1+\tfrac{7}{16}\kappa^2+O(\kappa^4, k^{-1})\} \quad (k\to\infty). \tag{8.7}$$

Substituting (8.2) into (6.7), we obtain

$$|F^{(2)}(\alpha)|^2 = \exp(-2|\alpha|) + \epsilon k K_1(2k) \exp(-|\alpha|) \cosh \alpha + O(\epsilon^2) \quad (|\alpha| < k). \tag{8.8}$$

Substituting (8.8) into (3.3*b*), we obtain

$$C_D = C_{D1}\{1 + \tfrac{1}{2}\epsilon k K_1(2k)\} + \tfrac{1}{3}\pi\epsilon^2 k^4 K_1(2k) + O(\epsilon^3), \tag{8.9}$$

where C_{D1} is given by (8.3), and K_1 is a modified Bessel function of the second kind. The result (8.9) is plotted in figure 7. We emphasize that it is not uniformly valid as $k \to \infty$, in which limit the terms of $O(\epsilon)$ are exponentially small.

9. Rectangular obstacle

We illustrate the effect of discontinuities in height by considering the extreme case of a rectangular obstacle [Lyra (1943) gave the wave patterns for this obstacle but did not calculate the wave drag]. Substituting

$$\eta(x) = H(1-|x|), \quad \eta'(x) = \delta(1+x) - \delta(1-x) \tag{9.1a, b}$$

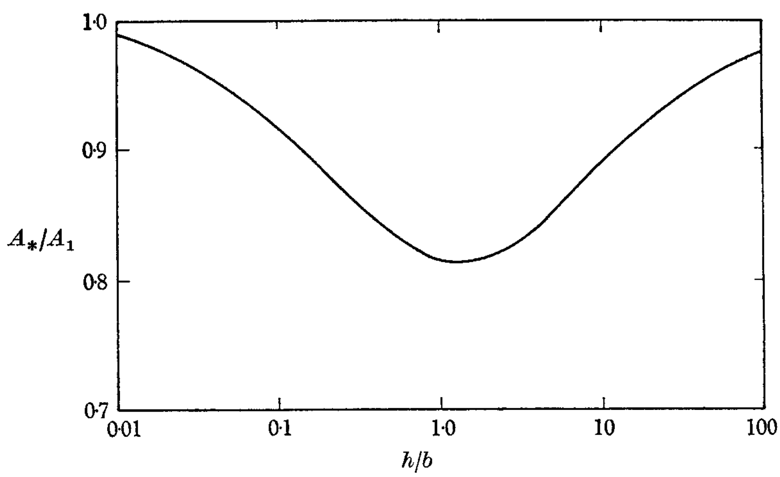

FIGURE 8. The dipole form of a rectangular obstacle, as given by (A 5).

into (3.8), we obtain (after some reduction)

$$C_{D1} = 2\kappa \int_0^{2\kappa} x^{-1} \mathbf{H}_1(x)\, dx \quad (\epsilon \to 0) \tag{9.2a}$$

$$= \epsilon \sum_{n=0}^{\infty} (-)^n [(n+1)\Gamma(n+\tfrac{3}{2})\Gamma(n+\tfrac{5}{2})]^{-1} k^{2n+3} \tag{9.2b}$$

$$\sim (4\kappa/\pi)(\gamma + \log 4k - 1) \quad (k \to \infty) \tag{9.2c}$$

as the first-order approximation to the drag coefficient; $\mathbf{H}_1$ is a Struve function. The result (9.2*b*) is plotted in figures 2 and 3.

The dipole form for the rectangular obstacle is given by (A 5) in appendix A and is plotted in figure 8.

The Hilbert transform of (9.1 *a*) is

$$\eta_* = -\frac{1}{\pi}\log\left|\frac{1+x}{1-x}\right|. \tag{9.3}$$

Substituting (9.1 *a*) and (9.3) into (5.12 *b*) and (5.11 *a*), we obtain

$$\zeta(x) = \operatorname{cosec}\kappa\left[\left|\frac{1+x}{1-x}\right|^{\kappa/\pi} - H(1-|x|)\cos\kappa - H(|x|-1)\right] \tag{9.4}$$

and

$$f(x) = \left(\frac{1+x}{1-x}\right)^{\kappa/\pi} \quad (|x| < 1). \tag{9.5}$$

We infer from (9.4) and (5.14) that $\kappa_c \to 0$ as $k \to \infty$ in consequence of the discontinuity in $\eta(x)$ at $x = 1$. The anomalous behaviour of C_D implied by (9.2 *c*) as $k \to \infty$ is therefore of rather limited interest.

This work was partially supported by the National Science Foundation under Grant GA-849, by the Office of Naval Research under Contract Nonr-2216(29), and by a Sydney University Post-Graduate Travelling Fellowship (H.E.H.).

Appendix A. Dipole-form examples

The following examples are summarized in table 1. They are based on results that are either well known (see, e.g. Milne-Thomson 1960) or may be regarded as straightforward exercises in potential theory. We emphasize that they are offered primarily in support of the approximation (4.14) and are not necessarily of direct physical interest.

Circular-arc mound or ditch

Circular-arc mounds of base $2b$ and height

$$h = b\tan\tfrac{1}{2}\alpha\pi \quad (-1 < \alpha < 1), \tag{A 1}$$

with α as the family parameter,† permit the determination of w in co-axal co-ordinates; we obtain

$$A_1 = \tfrac{1}{3}\alpha(2-\alpha)(1-\alpha)^{-2}b^2. \tag{A 2}$$

Negative values of α yield ditches, for which we must regard A as negative and (4.14) as inapplicable. The validity of the calculation for a real fluid is especially questionable for $|\alpha| > \frac{1}{2}$.

Letting $\alpha \to 0$ (shallow mound or ditch), we obtain

$$A_1 = (\tfrac{2}{3}\alpha + \alpha^2 + \tfrac{4}{3}\alpha^3 + \ldots)b^2 \tag{A 3a}$$

and

$$A_* = \left(\tfrac{2}{3}\alpha + \tfrac{1}{8}\pi^2\alpha^2 + \frac{4\pi^2}{45}\alpha^3 + \ldots\right)b^2. \tag{A 3b}$$

Letting $\alpha = \frac{1}{2}$, we recover a semi-circle of radius $a = h = b$. Letting $\alpha \to 1$, we obtain a full circular obstacle of radius $a = b/(1-\alpha)\pi$, such that

$$A_1 \to \tfrac{1}{3}\pi^2a^2 \equiv \tfrac{1}{9}\pi^2A_* \quad (\alpha \to 1). \tag{A 4}$$

† The parameter α, as used in this section, has no connexion with the wave number in §2 above.

Numerical calculations reveal that (A_*/A_1) oscillates about unity (thereby proving that A_* is neither an upper or lower bound to A_1) in $\alpha = (0, 1)$ with a maximum deviation of roughly 10 % at $\alpha = 1$ and of roughly 5 % in $\alpha = (0, \frac{3}{4})$.

Letting $\alpha = -\frac{1}{2}$, we obtain a semi-circular ditch of radius $a = h = b$, for which $A_1 = -5a^2/27$ and the wave drag (as $k \to 0$) is roughly $3\frac{1}{2}$ % of that for a semi-circular mound of radius a. Letting $\alpha \to -1$, we obtain a circular ditch with an opening of approximately $(1+\alpha)$ times its circumference and a drag proportional to $(1+\alpha)^4$ for fixed radius.

The limiting case of a full circular obstacle provides a fairly extreme test for the bounds of (4.13). Choosing the inner ellipse as a vertical plate ($h_i = 2a$, $b_i = 0$) and an outer ellipse that has matching ordinate, slope, and curvature at the summit ($h_0 = 2a$, $b_0 = 2^{\frac{1}{2}}a$), we obtain $A_{1i} = 2a^2$ and $A_{10} = (2+2^{\frac{1}{2}})a^2$. The lower bound is understandably poor, but the upper bound is only 4 % high.

Rectangular obstacle

The complex potential for a rectangular obstacle of width $2b$ and height h may be obtained through a Schwarz–Christoffel transformation, which yields the parametric results

$$b = lf(\kappa), \quad h = lf(\sqrt{(1-\kappa^2)}), \quad A_1 = \tfrac{1}{2}(1-\kappa^2)l^2, \qquad (\text{A } 5a, b, c)$$

where

$$f(\kappa) = E(\kappa) - (1-\kappa^2)K(\kappa) \quad (0 < \kappa < 1), \qquad (\text{A } 6)$$

and E and K are complete elliptic integrals.

The ratio A_*/A_1, which is plotted in figure 8, tends to unity as either $h/b \to 0$ or $b/h \to 0$ and exhibits a maximum departure from unity of roughly 20 %. In particular, $A_1 = 1{\cdot}40h^2$ and $A_* = 1{\cdot}14h^2$ for $h = b$. The corresponding lower and upper bounds obtained by inscribing and circumscribing semi-circles are $A_i = h^2$ and $A_0 = 2h^2$; circumscribing a semi-ellipse and adjusting h_0/b_0 to minimize A_0, we obtain $A_0 = 1{\cdot}81h^2$ (for $h_0 = 0{\cdot}655b_0$).

The most interesting special cases are given by

$$A_1 = \tfrac{1}{2}h^2 + (A/2\pi)\{\log(4\pi h/b) - 1\} + O\{b^2 \log(h/b)\} \quad (b/h \to 0) \qquad (\text{A } 7)$$

and

$$A_1 = \pi^{-1}A + (2h^2/\pi^2)\{\log(4\pi b/h) + \tfrac{1}{2}\} + O\{(h^3/b)\log(b/h)\} \quad (h/b \to 0). \qquad (\text{A } 8)$$

These results evidently do tend to (4.14), but only very slowly, as either b/h or h/b tends to zero. We infer from (A 8) that $\frac{1}{2}\pi h^2$ is not even a qualitatively valid approximation to the virtual mass M as $h/b \to 0$. We contrast this with the qualitatively valid implication of (A 3) for a circular-arc mound, namely that $M \to \frac{1}{2}\pi h^2 . (8/\pi^2)$ as $\alpha \to 0$.

Lemniscate

The lemniscate of Bernoulli provides an example of an obstacle with an intermediate valley. Choosing $2l$ as the distance between foci, we obtain

$$r^2 = 2\cos 2\theta \quad (0 \leqslant \theta \leqslant \pi) \qquad (\text{A } 9)$$

as the profile in polar co-ordinates. The corresponding height and area are $h = \frac{1}{2}l$ and $A = l^2$. The determination of the complex potential [Miles & Backus

1968; the solution given by Basset (1888, §§114, 117) in his treatise is incorrect] yields $A_1 = \frac{1}{2}l^2$. Combining these results, we obtain

$$A_1 = 2h^2 = \tfrac{1}{2}A, \quad A_* = \{\tfrac{1}{2}+(4/\pi)\}h^2. \qquad \text{(A 10}a, b)$$

We add that the bounds of (4.13) are poor in consequence of the valley in C.

Joukowsky profile

Airfoils provide convenient examples of asymmetric obstacles. We consider the Joukowsky profile obtained from a circle of radius l with centre at $\zeta = \epsilon l$ in the complex ζ-plane, namely

$$z = \zeta + (1-\epsilon)^2\zeta^{-1}, \quad |\zeta - \epsilon| = 1. \qquad \text{(A 11}a, b)$$

Invoking the well-known solution for the flow around the circle, we obtain

$$A_1 = \epsilon(2-\epsilon)\,l^2. \qquad \text{(A 12)}$$

The area is given by $A = 2\pi\epsilon l^2/(1+\epsilon)^2$, but $h(\epsilon)$ is a rather complicated, algebraic expression. A typical case is $\epsilon = \frac{1}{2}$, for which $A = 1{\cdot}39l^2$, $h = 0{\cdot}81l$, $A_1 = 0{\cdot}75l^2$, and $A_* = 0{\cdot}77l^2$. Numerical calculations for other ϵ in $(0, 1)$ reveal that A_*/A_1 exhibits deviations similar to those for a circular arc and tends to unity at $\epsilon = 1$, where the profile becomes a semi-circle.

Finned semi-circle

A rather extreme example is provided by a thin, vertical plate of height $h-a$ mounted on top of a semi-circular obstacle (so that the overall height is h). Mapping this configuration on the unit circle, we obtain

$$A_1 = \tfrac{1}{2}(h^2 + a^4h^{-2}) \qquad \text{(A 13)}$$

and

$$\frac{A_*}{A_1} = \frac{1+(a/h)^2}{1+(a/h)^4}. \qquad \text{(A 14)}$$

The latter ratio has a maximum value of $1{\cdot}207$ at $a/h = 0{\cdot}645$. Circumscribing an ellipse ($b_0 = a$, $h_0 = h$), we find that $A_{10} > A_* > A_1$ for all a/h.

We infer from the preceding examples, as summarized in table 1, that the approximation (4.14) to the dipole form A_1 is likely to be within 20 % of the correct value and is typically, although not always, a better approximation than either of the bounds of (4.13).

Appendix B. Channel of finite height

We consider the modification of the preceding formulation for a channel of finite height H. Choosing H/π, rather than b, as the characteristic length, we replace (1.1) by

$$\beta = \pi b/H, \quad \epsilon = \pi h/H, \quad k = NH/\pi U, \quad \kappa = k\epsilon = Nh/U. \qquad \text{(B 1}a\text{–}d)$$

We also replace (1.5) by the two boundary conditions

$$\delta(x, \pi) = 0 \qquad \text{(B 2)}$$

and

$$\delta(x, y) \to 0 \quad (x \to -\infty). \qquad \text{(B 3)}$$

Proceeding as in §2, we take the finite-sine transform of (1.3) over $y = (0, \pi)$, invoke (2.4a) at $y = 0$ and (B 2) at $y = \pi$, require the transform to satisfy (B 3), and invert the result to obtain [cf. (2.1a)]

$$\pi\delta(x,y) = \int_{-\infty}^{\infty} f(\xi)\,\delta_1(x-\xi)\,d\xi, \tag{B 4}$$

where [cf. (2.18)]

$$\delta_1(x,y) = -2H(x)\sum_{n=1}^{K}(n/k_n)\sin(k_n x)\sin ny + \sum_{n=K+1}^{\infty}(n/\alpha_n)\exp(-\alpha_n|x|)\sin ny, \tag{B 5}$$

$$k_n = (k^2-n^2)^{\frac{1}{2}}, \quad \alpha_n = (n^2-k^2)^{\frac{1}{2}}, \quad K < k < K+1, \tag{B 6a,b,c}$$

and K is the integral part of k. The dipole solution (B 5) is identical with that given originally by Drazin & Moore [1967, equation (5.7) with $\mu = \pi$ therein].

Substituting (B 5) into (B 4) and letting $x \to \infty$, we obtain the lee-wave field

$$\delta(x,y) \sim -(2/\pi)\sum_{n=1}^{K}(n/k_n)\sin ny\int_{-\infty}^{\infty} f(\xi)\sin\{k_n(x-\xi)\}\,d\xi \quad (x\to\infty). \tag{B 7}$$

The lee-wave drag is given by [Drazin & Moore's equation (5.8) contains a numerical error]

$$D = (\epsilon^2 qH/\pi)\int_0^{\pi}(\delta_x^2-\delta_y^2+k^2\delta^2)\,dy \quad (x > 0). \tag{B 8}$$

Substituting (B 7) into (B 8), dividing by qh, and carrying out the y integration (we note that the contributions of the exponentially damped modes would have vanished identically at this stage if the integration had been carried out for any positive value of x), we obtain

$$C_D = 2\pi\epsilon\sum_{n=1}^{K} n^2|F(k_n)|^2, \tag{B 9}$$

where F is the Fourier transform defined by (2.3).

In the planar approximation, $\epsilon \to 0$, we obtain (2.5), just as for the half-space. We emphasize that, under the present normalization, $\eta(x)$ is the ratio of the obstacle height at a point Hx/π from the origin to the maximum height h.

We now consider the Rayleigh-scattering approximation, for which each of β, ϵ, and κ, as defined by (B 1a, b, d), must be small. Remarking that the range of integration in (2.3) is over $x = O(\beta)$, we obtain

$$F(k_n) \to F_0 \equiv \pi A_1/Hh \quad (\beta\to 0), \tag{B 10}$$

where A_1 is the dipole form of C, defined precisely as in §4 (the effect of the upper channel wall is negligible in the Rayleigh-scattering approximation to the drag by virtue of the restriction $\epsilon \ll 1$). Substituting (B 10) into (B 9) and summing the series, we obtain

$$D \to \tfrac{2}{3}\pi K(K+\tfrac{1}{2})(K+1)(\pi/H)^3 A_1^2 q \quad (\beta\to 0). \tag{B 11}$$

Letting $H \to \infty$ while holding b fixed, so that $K\to\infty$ and $(\pi K/H) \to (N/U)$, we recover (4.8).

The limit $k\to\infty$ with β fixed implies that the channel may be approximated by a half-space, in which case the problem reduces to that considered in §5 if κ also is fixed.

REFERENCES

Archibald, P. C. & Court, N. A. 1964 Curves. *Encyclopedia Brittanica.*

Basset, A. B. 1888 *A Treatise on Hydrodynamics* (1961 reprint). New York: Dover.

Blumen, W. 1965 A random model of momentum flux by mountain waves. *Geofys. Publ.* **26**, no. 2.

Colson, J. 1801 *Analytical Institutions.* London: Taylor and Wilkes.

Drazin, P. G. & Moore, D. W. 1967 Steady two-dimensional flow of a fluid of variable density over an obstacle. *J. Fluid Mech.* **28**, 353–70.

Erdélyi, A., Magnus, W., Oberhettinger, F. & Tricomi, F. G. 1953*a* *Higher Transcendental Functions*, vols. 1 and 2. New York: McGraw-Hill.

Erdélyi, A., Magnus, W., Oberhettinger, F. & Tricomi, F. G. 1953*b* *Tables of Integral Transforms*, vols. 1 and 2. New York: McGraw-Hill.

Grandi, G. 1718 Note al trattato del Galileo del moto naturale accellerato. *Opere di Galileo Galilei*, vol. 3. Firenze.

Huppert, H. E. & Miles, J. W. 1969 Lee waves in a stratified flow. Part 3. Semi-elliptical obstacle. *J. Fluid Mech.* **35**, 481.

Lamb, H. 1932 *Hydrodynamics.* Cambridge University Press.

Lyra, G. 1943 Theorie der stationären Leewellenströmung in freier Atmosphäre. *Z. angew. Math. Mech.* **23**, 1–28.

Miles, J. W. 1968*a* Lee waves in stratified flow. Part 1. Thin barrier. *J. Fluid Mech.* **32**, 549–68.

Miles, J. W. 1968*b* Lee waves in stratified flow. Part 2. Semi-circular obstacle. *J. Fluid Mech.* **33**, 803–14.

Miles, J. W. & Backus, G. E. 1968 On the potential flow past a lemniscate and a general method of Milne-Thomson. *Quart. Appl. Math.* **26**, 441–2.

Milne-Thomson, L. M. 1960 *Theoretical Hydrodynamics.* New York: Macmillan.

Mushkelishvili, N. I. 1953 *Singular Integral Equations.* Groningen: P. Noordhoff.

Pölya, G. 1947 A minimum problem about the motion of a solid through a fluid. *Proc. Nat'l. Acad. Sci.* **33**, 218–21.

Pölya, G. & Szegö, G. 1951 *Isoperimetric Inequalities in Mathematical Physics.* Princeton University Press.

Queney, P. 1948 The problem of airflow over mountains. *Bull. Amer. Meteor. Soc.* **29**, 16–26.

Rayleigh, Lord 1897 On the incidence of aerial and electric waves upon small obstacles in the form of ellipsoids. *Phil. Mag.* **44**, 28–52; *Scientific Papers*, **4**, 305–26.

Sawyer, J. S. 1959 The introduction of the effects of topography into numerical forecasting. *Quart. J. R. Met. Soc.* **85**, 31–43.

Titchmarsh, E. C. 1948 *Introduction to the Theory of Fourier Integrals.* Oxford University Press.

Van Dyke, M. D. 1964 *Perturbation Methods in Fluid Mechanics.* New York: Academic Press.

Ward, G. N. 1955 *Linearized Theory of High Speed Flow.* Cambridge University Press.

Yih, C.-S. 1965 *Dynamics of Nonhomogeneous Fluids.* New York: Macmillan.